

# Ultra-highly sensitive HCl-LITES sensor based on a low-frequency quartz tuning fork and a fiber-coupled multi-pass cell

Shunda Qiao<sup>a</sup>, Angelo Sampaolo<sup>b</sup>, Pietro Patimisco<sup>b</sup>, Vincenzo Spagnolo<sup>b</sup>, Yufei Ma<sup>a,\*</sup>

<sup>a</sup> National Key Laboratory of Science and Technology on Tunable Laser, Harbin Institute of Technology, Harbin 150001, China

<sup>b</sup> PolySense Lab, Dipartimento Interateneo di Fisica, University and Politecnico of Bari, Via Amendola 173, Bari, Italy

## ARTICLE INFO

### Keywords:

Hydrogen chloride  
Quartz tuning fork  
Multi-pass cell  
Gas sensing  
Light-induced thermoelastic spectroscopy

## ABSTRACT

In this paper, an ultra-highly sensitive light-induced thermoelastic spectroscopy (LITES) based hydrogen chloride (HCl) sensor, exploiting a custom low-frequency quartz tuning fork (QTF) and a fiber-coupled multi-pass cell (MPC) with optical length of 40 m, was demonstrated. A low resonant frequency of 2.89 kHz of QTF is advantageous to produce a long energy accumulation time in LITES. Furthermore, the use of an MPC with the fiber-coupled structure not only avoids the difficulty in optical alignment but also enhances the system robustness. A distributed feedback (DFB) diode laser emitting at 1.74  $\mu\text{m}$  was used as the excitation source. Under the same operating conditions, the using of low-frequency QTF provided a  $\sim 2$  times signal improvement compared to that achieved using a standard 32 kHz QTF. At an integration time of 200 ms, a minimum detection limit (MDL) of 148 ppb was achieved. The reported sensor also shows an excellent linear response to HCl gas concentration in the investigated range.

## 1. Introduction

As the main source of dioxin, hydrogen chloride (HCl) is an air pollution gas [1,2]. HCl existing in the atmosphere comes primarily from the waste emission of incineration plants and chemical plants [3,4]. Therefore, for atmosphere pollution control, it has great significance to monitor the content of HCl in the air and waste gases. Furthermore, HCl is used in various fields, such as plasma etching [5], photochemistry [6] and semiconductor manufacturing [7]. Inhalation of HCl fumes can cause choking, inflammation of the upper respiratory tract, and in severe cases, pulmonary edema, circulatory system failure, and death. HCl is also highly corrosive, thereby there is to a great demand for sensitive and accurate monitoring of HCl concentration for safety reasons.

Up to now, many kinds of HCl sensors by employing optical, chemical, or electrical methods have been reported [8–12]. Among them, laser absorption spectroscopy (LAS) stands out due to its merits of high sensitivity, excellent selectivity and rapid response [13–16]. Tunable diode laser absorption spectroscopy (TDLAS) has been employed for the detection of HCl and with an averaging time of 1 s, a 2 ppm detection sensitivity was achieved [17]. In TDLAS, a photoelectric detector is used to measure the variation of light intensity. However, photoelectric detector usually has a high price. Furthermore, at some specific

wavelength range such as the long wave region of  $> 10 \mu\text{m}$ , it is hard to acquire an available photoelectric detector.

In 2002, quartz-enhanced photoacoustic spectroscopy (QEPAS) was reported for the first time [18]. A low-cost and wavelength independence quartz tuning fork (QTF) is employed as an acoustic wave transducer to measure the photoacoustic signal produced by target gas [19–23]. The tiny size and high-quality factor of QTF make QEPAS system compact and immune to the background noise [24–28]. Ma et al. recently reported a sensitive QEPAS based HCl sensor [29], at an integration time of 1 s, reaching a minimum detection limit (MDL) of 550 ppb. Nevertheless, in QEPAS, the QTF must be placed into the target analyte which means that QEPAS technique is unsuitable to detect acid and corrosive gases such as HCl because the QTF and the deposited silver contact pattern could be corroded for long-term exposure, resulting in a rapid sensor failure.

In 2009, a QTF was used as the detector of electromagnetic radiation for the first time which was reported by Pohlkötter et al. [30]. Then a novel QTF-based sensitive trace gas detection technique called Light-induced thermoelastic spectroscopy (LITES) was proposed by Ma et al. in 2018 [31]. In LITES, the laser hits the surface of the QTF after passing through the target gas sample. The gas partially absorbs the laser beam, and then the residual energy absorbed by the QTF is converted

\* Corresponding author.

E-mail address: [mayufei@hit.edu.cn](mailto:mayufei@hit.edu.cn) (Y. Ma).

<https://doi.org/10.1016/j.pacs.2022.100381>

Received 20 April 2022; Received in revised form 14 June 2022; Accepted 15 June 2022

Available online 17 June 2022

2213-5979/© 2022 The Author(s). Published by Elsevier GmbH. This is an open access article under the CC BY-NC-ND license (<http://creativecommons.org/licenses/by-nc-nd/4.0/>).

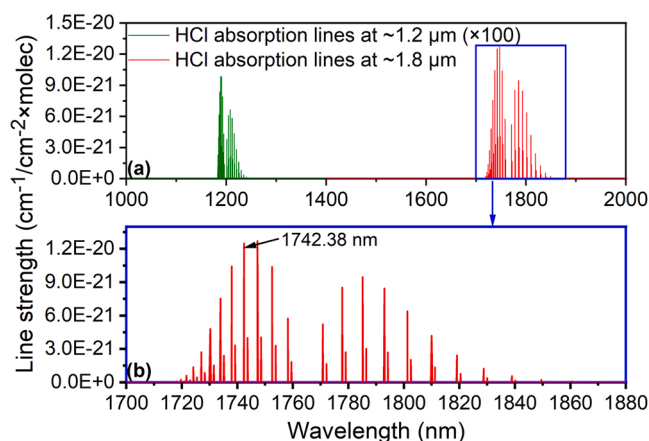


**Fig. 1.** (a) Simulation of HCl absorption lines located in the near-IR spectral range according to the HITRAN 2016 database. (b) HCl absorption lines around 1.8  $\mu\text{m}$ .

into thermal energy, resulted in a thermoelastic expansion of QTF. If the laser intensity is modulated, the QTF will suffer mechanical vibration at the modulation frequency and these vibrations are enhanced when the QTF operates in resonance conditions. LITES is a non-contact technique in which there is no need to place the QTF into the detected gases [32–35]. Therefore, this technique not only keeps the merits of QEPAS but also can be employed for detection of acid and corrosive gases. In 2021, Ma et al. reported a HCl gas sensor by employing the LITES technique. With an integration time of 1 s, an MDL of  $\sim 420$  ppb was achieved [36]. As an important detection unit, QTF has a great influence on the performance of both QEPAS and LITES sensor systems. At present, the most commonly used QTF is the standard commercially available ones with a resonant frequency of  $\sim 32$  kHz. However, such a high frequency leads to a short energy accumulation time of the system. A higher resonant frequency of QTF means the system will have a shorter modulation period. Therefore, in one modulation cycle, the QTF will be irradiated by the laser for a shorter time, which will make the QTF absorb less laser energy and expand less drastically, so as to produce a weaker piezoelectric signal. Therefore, to achieve a more sensitive detection, the use of low-frequency QTFs as the detector is an effective way [37–40].

In this paper, an ultra-highly sensitive HCl-LITES sensor based on a custom low-frequency QTF is reported for the first time. A fiber-coupled multi-pass cell (FC-MPC) with an effective optical length of 40 m was employed in the system to improve the sensor performance by increasing the gas absorption pathlength. Compared with the commonly

used spatially coupled MPC, the fiber-coupled structure reduces the difficulty in optical alignment as well as ensures excellent system robustness. Moreover, wavelength modulation spectroscopy (WMS) and the second harmonic demodulation techniques were exploited to reduce background noise.

## 2. Experimental setup

### 2.1. Diode laser characterization

The mid-infrared spectral region is the fundamental absorption band for most gases with a strong absorption strength. However, compared with the mid-infrared excitation sources, such as quantum cascade lasers (QCLs) or interband cascade lasers (ICLs), near-infrared diode lasers emitting at wavelength of less than 3  $\mu\text{m}$  shows several advantages of compactness, low-cost and stable output characteristics, which thus is more suitable for adopting in the sensor system. Therefore, in this research, a distributed feedback (DFB) fiber-coupled diode laser was employed as the light source. According to the HITRAN 2016 database [41], the line strength of HCl located below 3  $\mu\text{m}$  are simulated and shown in Fig. 1(a).

It can be seen the absorption band located at  $\sim 1.8$   $\mu\text{m}$  is stronger than that around 1.2  $\mu\text{m}$ . Thereby, to obtain a good detection performance an absorption line located at 1742.38 nm ( $5739.27$   $\text{cm}^{-1}$ ) was selected as absorption feature to be targeted (see Fig. 1(b)).

The output characteristics of the employed diode laser was investigated at first. With different operating temperatures, the measured laser wavenumber as a function of driving current is plotted in Fig. 2(a). The laser output power as a function of the driving current is shown in Fig. 2(b). During the experiment, the laser temperature was set at 24.5  $^{\circ}\text{C}$ . For the laser emission wavelength matching the selected absorption line, the optical power resulted 12.3 mW and a good 2D Gaussian beam profile was measured by utilizing a pyrocamera (PyrocamTM IIIHR, Ophir) and shown in the inset of Fig. 2(b).

### 2.2. Sensor configuration

A schematic of the experimental HCl-LITES sensor setup, exploiting a fiber-coupled multi-pass cell (MPC), is depicted in Fig. 3. By employing a fiber coupler, the diode laser beam was coupled into the fiber coupled-MPC (FC-MPC) and, after several reflections, the light comes out from the exit hole. An effective optical length of 40 m was achieved. When the MPC was filled with pure  $\text{N}_2$ , a 2D beam profile of the output laser beam from FC-MPC at the target wavelength was also measured by employing a pyrocamera and shows a good beam profile quality. After passing through the FC-MPC, the laser beam was collimated by using a fiber

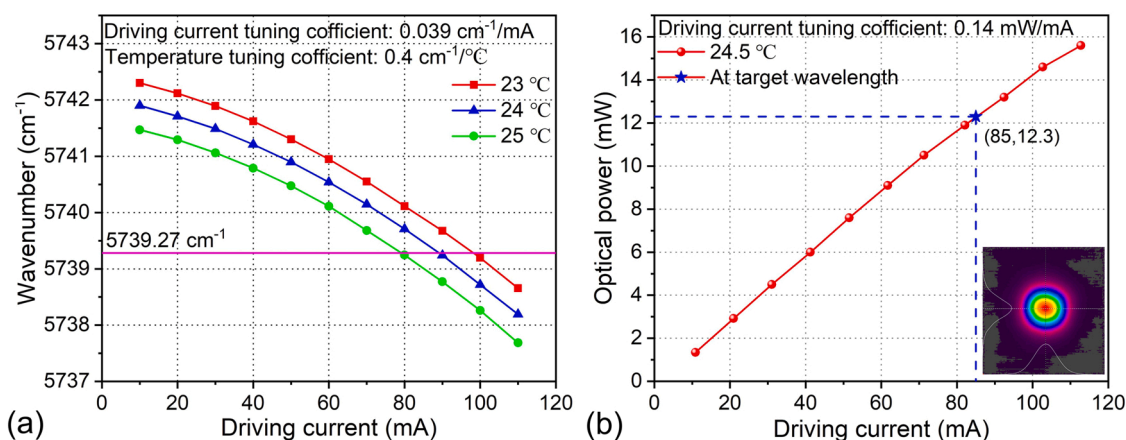


**Fig. 2.** Output performance of 1.74  $\mu\text{m}$  DFB fiber-coupled laser: (a) Laser wavenumber as a function of driving current with different operating temperatures. (b) Laser output power as a function of driving current at 24.5  $^{\circ}\text{C}$ . Inset: 2D laser beam profile for a driving current of 85 mA.

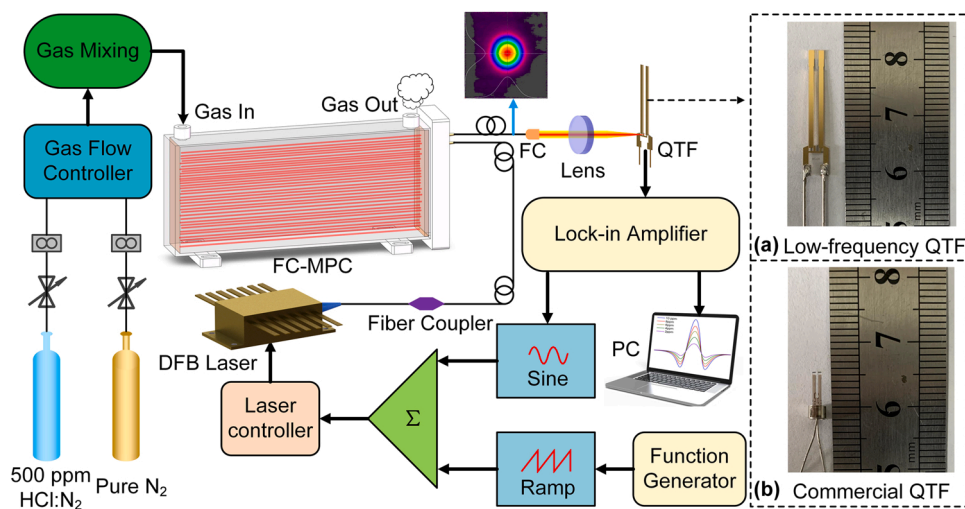


Fig. 3. Schematic configuration of the HCl-LITES sensor. DFB, distributed feedback; FC-MPC, fiber-coupled multi-pass cell; FC, fiber collimator; QTF, quartz tuning fork; PC, personal computer. (a) Diagram of the low-frequency QTF. (b) Diagram of the commercial 32 kHz QTF.

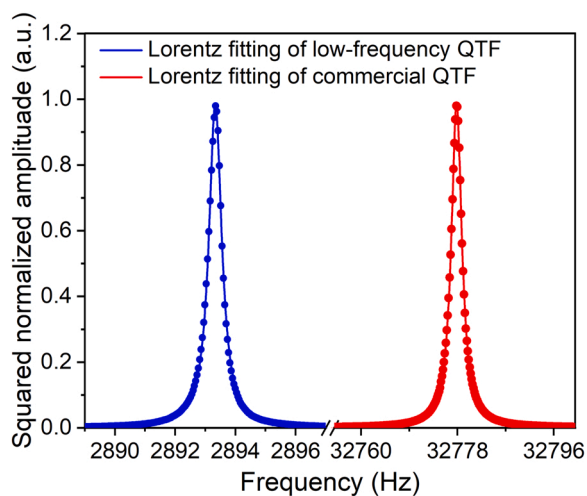


Fig. 4. Frequency response for the low-frequency QTF (blue line) and the commercial QTF (red line), respectively.

collimator (FC) at first and was ultimately focused on the base of the QTF prongs, where the strongest LITES signal is expected [21]. In the system, the focal length of the used lens is 30 mm. At this condition, the optical power was measured as 2.57 mW at the target wavelength. For comparison, two QTFs were employed: a low-frequency custom QTF and a commercial 32 kHz QTF. Pictures of two QTFs is shown in Fig. 3(a) and (b), respectively. Starting from a 500 ppm HCl:N<sub>2</sub> certified mixture and by using two gas flow controllers with the accuracy of  $\pm 1\%$  at full scale, different mixing ratio of HCl was generated as gas samples to determine the sensor performance. To reduce the background noise, wavelength modulation spectroscopy (WMS) and the 2nd harmonic detection techniques were employed. A function generator provided a ramp wave was used to scan the laser wavelength across the target absorption line with the scanning time of 200 s. A lock-in amplifier generated a sine wave was employed for laser wavelength modulation and as the reference signal for demodulation. In one modulation period, the laser wavelength will pass through the gas absorption peak twice, therefore, in order to achieve the best resonance state of QTF, the wavelength modulation frequency was set at half of its resonant frequency. When the integration time of the system was set at 200 ms, the  $2f$  component of LITES signal was demodulated by the lock-in amplifier with a detection bandwidth of 345.4 mHz.

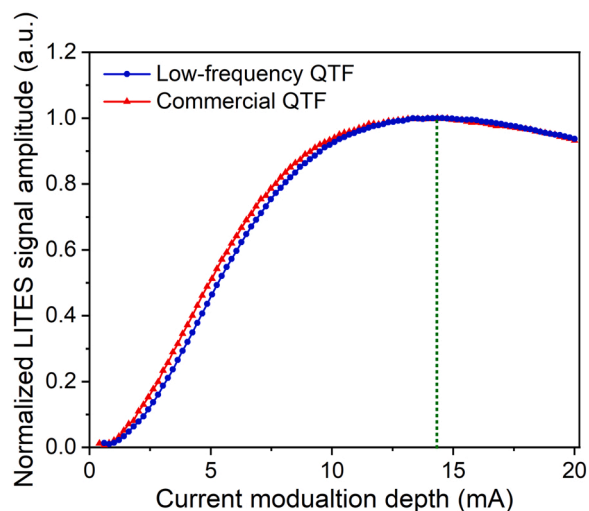


Fig. 5. LITES signal amplitude as a function of current modulation depth for the systems using the low-frequency QTF (blue line) and the commercial QTF (red line), respectively.

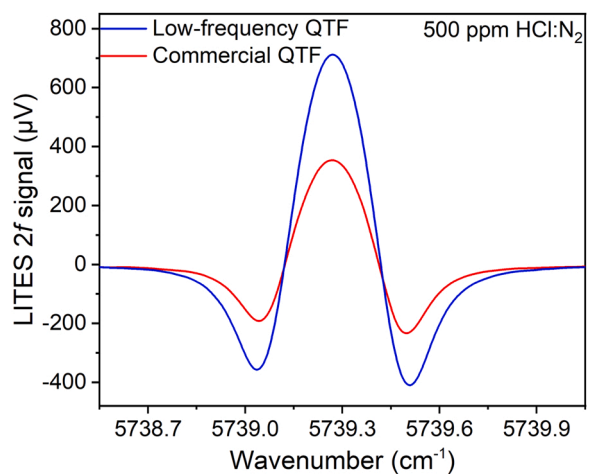


Fig. 6.  $2f$  LITES signal for two different QTFs at the same experimental conditions.

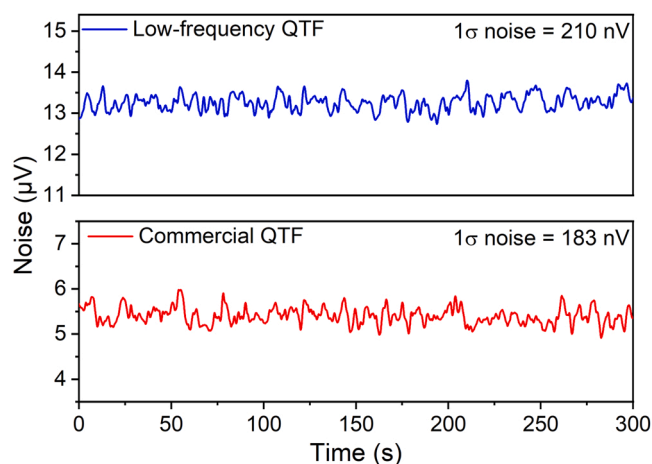


Fig. 7. System noise measured with the two different QTFs with a 200 ms integration time.

### 3. Experimental results and discussion

The characteristic of the two QTFs was measured firstly to extract the resonance frequencies and the related quality factors. The QTFs frequency response is shown in Fig. 4. The data were normalized and fitted with a Lorentz function. A resonant frequency ( $f$ ) of 2893.3 Hz and 32,777.8 Hz with detection bandwidths of  $\Delta f_1 = 0.49$  Hz and  $\Delta f_2 = 2.35$  Hz were extracted for the low-frequency custom QTF and the commercial QTF, respectively. According to the formula of  $Q = f/\Delta f$ , the related quality factors resulted 5904 and 13,948, respectively.

In WMS technique, modulation depth is an important parameter that should be optimized to obtain a strong LITES signal. The dependence of the LITES signal amplitude as a function of current modulation depth is shown in Fig. 5. For comparison, the signal amplitude was normalized for both QTFs. For both cases, at a current modulation depth of 14.3 mA the LITES signal reached its maximum value.

Under the same operating conditions, the  $2f$  LITES signals using the two different QTFs were measured for a 500 ppm HCl:N<sub>2</sub> gas mixture. As shown in Fig. 6, the  $2f$  signal amplitudes resulted 711.6  $\mu$ V and 353.4  $\mu$ V for the low-frequency QTF and the commercial QTF, respectively. Obviously, the signal detected by using the low-frequency QTF resulted  $\sim 2$  times higher with respect to that measured when employing the commercial QTF. Such a high improvement is mainly due to the low resonant frequency of the custom QTF, which is beneficial in term of increasing of the energy accumulation time for LITES technique.

The background noise of the systems employing two different QTFs

was also measured. The laser wavelength was locked at the peak of the selected HCl absorption line. Then, the  $2f$  signal amplitude was monitored continuously for 300 s while the FC-MPC was filled of pure N<sub>2</sub>. Fig. 7 shows the measured noise signal. The  $1\sigma$  noise resulted 210 nV and 183 nV for the low frequency and the commercial QTF, respectively. The MDL can be calculated by dividing the target gas concentration by the signal-to-noise ratio of the system. So, the optimal HCl-LITES  $1\sigma$  MDL and  $3\sigma$  MDL were achieved by exploiting the low-frequency QTF and resulted to be 148 ppb and 444 ppb, respectively.

The response in HCl concentration with the low-frequency QTF-based sensor system was investigated. By using the gas flow controllers, 500 ppm HCl was diluted with pure N<sub>2</sub> to obtain different concentrations. With each HCl concentration, the  $2f$  LITES signal was measured as shown in Fig. 8(a). The signal peak values as a function of HCl concentrations are displayed in Fig. 8(b). The data were fitted with a linear function and an R-squared of 0.99 was obtained. The fitting results proved that, in the investigated concentration range, the system shows an excellent linear response vs HCl concentration. According to the  $3\sigma$  noise and the concentration linear response results of the system, the fluctuation of the reproducible quantification concentration is estimated to be 0.45 ppm.

### 4. Conclusion

In conclusion, a highly sensitive LITES-based HCl sensor exploiting a custom low-frequency QTF and a FC-MPC with an effective optical length of 40 m was demonstrated. The fiber-coupled structure reduces the difficulty in optical alignment as well as improves the system robustness. The employed excitation source was a DFB, fiber-coupled, near-infrared diode laser with a central emission wavelength of 1.74  $\mu$ m. A custom low-frequency QTF and a commercially available QTF were compared with the LITES setup. With a 500 ppm HCl, the use of low-frequency QTF allows a  $\sim 2$  times signal improvement if compared with that achievable with a commercial QTF. When the system integration time was set at 200 ms, the low-frequency QTF-based HCl-LITES sensor achieved an  $1\sigma$  MDL and  $3\sigma$  MDL of 148 ppb and 444 ppb, respectively. It was also verified that the reported sensor shows an excellent linear response to the HCl gas concentrations in the investigated range. This sensor performance makes it suitable for applications in environmental monitoring and chemical processing.

### Declaration of Competing Interest

The authors declare that they have no known competing financial interests or personal relationships that could have appeared to influence the work reported in this paper.

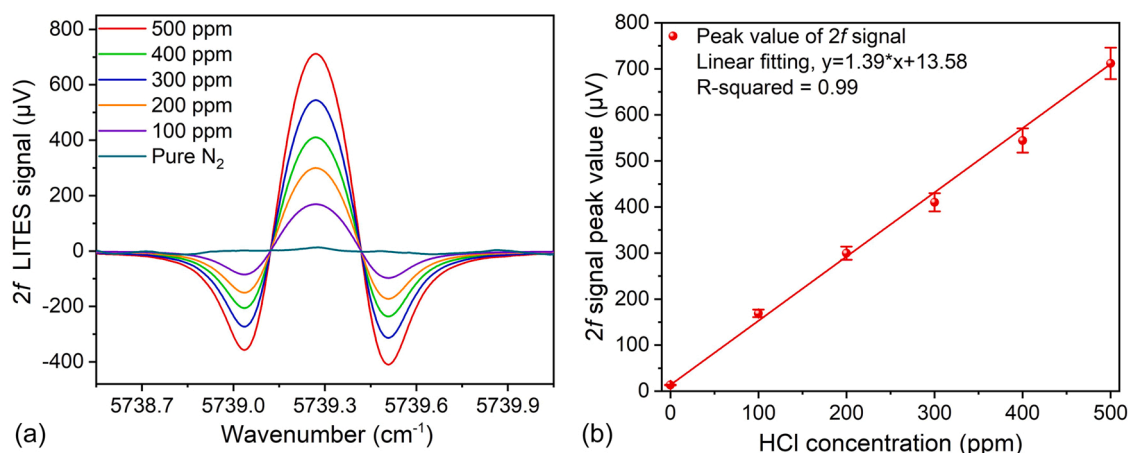


Fig. 8. (a)  $2f$  signal with different gas concentrations when the low-frequency QTF was used. (b)  $2f$  signal peak values as a function of gas concentrations.

## Data availability

Data will be made available on request.

## Acknowledgments

We are grateful for financial supports from the National Natural Science Foundation of China (Grant No. 62022032, 61875047 and 61505041), Natural Science Foundation of Heilongjiang Province of China (Grant No. YQ2019F006), Fundamental Research Funds for the Central Universities, Financial Grant from the Heilongjiang Province Postdoctoral Foundation (Grant No. LBH-Q18052). The authors from the physics department of Bari acknowledge financial support from THORLABS GmbH, within PolySense, a joint-research laboratory.

## References

- C.S. Chyang, Y.L. Han, L.W. Wu, H.P. Wan, H.T. Lee, Y.H. Chang, An investigation on pollutant emissions from co-firing of RDF and coal, *Waste Manag.* 30 (7) (2010) 1334–1340.
- T. Hatanaka, A. Kitajima, M. Takeuchi, Role of chlorine in combustion field in formation of polychlorinated dibenzo-p-dioxins and dibenzofurans during waste incineration, *Environ. Sci. Technol.* 39 (24) (2005) 9452–9456.
- B.E. Shemwell, A. Ergut, Y.A. Leventis, Economics of an integrated approach to control SO<sub>2</sub>, NO<sub>x</sub>, HCl, and particulate emissions from power plants, *J. Air Waste Manag.* 52 (5) (2002) 521–534.
- A.D. Pozzo, L. Lazazzara, G. Antonioni, V. Cozzani, Techno-economic performance of HCl and SO<sub>2</sub> removal in waste-to-energy plants by furnace direct sorbent injection, *J. Hazard. Mater.* 394 (2020), 122518.
- S. Kim, P. Klimecky, J.B. Jeffries, F.L. Terry, R.K. Hanson, In situ measurements of HCl during plasma etching of poly-silicon using a diode laser absorption sensor, *Meas. Sci. Technol.* 14 (9) (2003) 1662–1670.
- Y.B. Huang, Y.A. Yang, G.X. He, S. Hashimoto, R.J. Gordon, State resolved translational energy distributions of Cl and HCl in the ultraviolet photodissociation of chloroethylenes, *J. Chem. Phys.* 103 (13) (1995) 5476–5487.
- G. Melnychuk, H.D. Lin, S.P. Kotamraju, Y. Koshka, Effect of HCl addition on gas-phase and surface reactions during homoepitaxial growth of sic at low temperatures, *J. Appl. Phys.* 104 (5) (2008), 053517.
- M. Cano, P. Castillero, J. Roales, J.M. Pedrosa, S. Brittle, T. Richardson, A. R. Gonzalez-Elipse, A. Barranco, A transparent TmPyP/TiO<sub>2</sub> composite thin film as an hcl sensitive optochemical gas sensor, *Sens. Actuators B-Chem.* 150 (2) (2010) 764–769.
- Y.L. Tang, X.F. Xu, H.R. Du, H. Zhu, D.J. Li, D.Y. Ao, Y.J. Guo, Y.Q. Fu, X.T. Zu, Cellulose nano-crystals as a sensitive and selective layer for high performance surface acoustic wave HCl gas sensors, *Sens. Actuators A-Phys.* 301 (2020), 111792.
- L. Wang, R.V. Kumar, Thick film miniaturized HCl gas sensor, *Sens. Actuators B-Chem.* 98 (2) (2004) 196–203.
- Z.S. Li, Z.W. Sun, B. Li, M. Alden, M. Forsth, Spatially resolved trace detection of HCl in flames with mid-infrared polarization spectroscopy, *Opt. Lett.* 33 (16) (2008) 1836–1838.
- P. Ortwein, W. Woiwode, S. Fleck, M. Eberhard, T. Kolb, S. Wagner, M. Gisi, V. Ebert, Absolute diode laser-based in situ detection of HCl in gasification processes, *Exp. Fluids* 49 (4) (2010) 961–968.
- Y.F. Ma, Y.Q. Hu, S.D. Qiao, Y. He, F.K. Tittel, Trace gas sensing based on multi-quartz-enhanced photothermal spectroscopy, *Photoacoustics* 20 (2020), 100206.
- M.W. Sigrist, R. Bartlome, D. Marinov, J.M. Rey, D.E. Vogler, H. Waechter, Trace gas monitoring with infrared laser-based detection schemes, *Appl. Phys. B* 90 (2) (2008) 289–300.
- M.W. Sigrist, M. Naegele, A. Romann, Infrared laser spectroscopy for trace gas analysis, *Proc. SPIE* 4419 (2001) 14–17.
- Y.F. Ma, Y.Q. Hu, S.D. Qiao, Z.T. Lang, X.N. Liu, Y. He, V. Spagnolo, Quartz tuning forks resonance frequency matching for laser spectroscopy sensing, *Photoacoustics* 25 (2022), 100329.
- Z.C. Qu, J. Nwaboh, O. Werhahn, V. Ebert, Towards a TDLAS-based spectrometer for absolute HCl measurements in combustion flue gases and a better evaluation of thermal boundary layer effects, *Flow. Turbul. Combust.* 106 (2) (2021) 533–546.
- A.A. Kosterev, Y.A. Bakhrkin, R.F. Curl, F.K. Tittel, Quartz-enhanced photoacoustic spectroscopy, *Opt. Lett.* 27 (21) (2002) 1902–1904.
- Z.T. Lang, S.D. Qiao, Y.F. Ma, Acoustic microresonator based in-plane quartz-enhanced photoacoustic spectroscopy sensor with a line interaction mode, *Opt. Lett.* 47 (6) (2022) 1295–1298.
- Y.F. Ma, R. Lewicki, M. Razeghi, F.K. Tittel, QEPAS based ppb-level detection of CO and N<sub>2</sub>O using a high power CW DFB-QCL, *Opt. Express* 21 (1) (2013) 1008–1019.
- H.Y. Lin, H.D. Zheng, B.A.Z. Montano, H.P. Wu, M. Giglio, A. Sampaolo, P. Patimisco, W.G. Zhu, Y.C. Zhong, L. Dong, R.F. Kan, J.H. Yu, V. Spagnolo, Ppb-level gas detection using on-beam quartz-enhanced photoacoustic spectroscopy based on a 28 kHz tuning fork, *Photoacoustics* 25 (2022), 100321.
- Y. He, Y.F. Ma, Y. Tong, X. Yu, F.K. Tittel, HCN ppt-level detection based on a QEPAS sensor with amplified laser and a miniaturized 3D-printed photoacoustic detection channel, *Opt. Express* 26 (8) (2018) 9666–9675.
- H.P. Wu, L. Dong, H.D. Zheng, Y.J. Yu, W.G. Ma, L. Zhang, W.B. Yin, L.T. Xiao, S. T. Jia, F.K. Tittel, Beat frequency quartz-enhanced photoacoustic spectroscopy for fast and calibration-free continuous trace-gas monitoring, *Nat. Commun.* 8 (1) (2017) 1–8.
- J.P. Waclawek, H. Moser, B. Lendl, Compact quantum cascade laser based quartz-enhanced photoacoustic spectroscopy sensor system for detection of carbon disulfide, *Opt. Express* 24 (6) (2016) 6559–6571.
- M. Mordmüller, M. Köhring, W. Schade, U. Willer, An electrically and optically cooperated QEPAS device for highly integrated gas sensors, *Appl. Phys. B* 119 (1) (2015) 111–118.
- Z.T. Lang, S.D. Qiao, Y. He, Y.F. Ma, Quartz tuning fork-based demodulation of an acoustic signal induced by photo-thermo-elastic energy conversion, *Photoacoustics* 22 (2021), 100272.
- Y.F. Ma, W. Feng, S.D. Qiao, Z.X. Zhao, S.F. Gao, Y.Y. Wang, Hollow-core anti-resonant fiber based light-induced thermoelastic spectroscopy for gas sensing, *Opt. Express* 30 (11) (2022) 18836–18844.
- P. Patimisco, A. Sampaolo, L. Dong, F.K. Tittel, V. Spagnolo, Recent advances in quartz enhanced photoacoustic sensing, *Appl. Phys. Rev.* 5 (1) (2018), 011106.
- Y.F. Ma, Y. He, X. Yu, C. Chen, R. Sun, F.K. Tittel, HCl ppb-level detection based on QEPAS sensor using a low resonance frequency quartz tuning fork, *Sens. Actuators B* 233 (2016) 388–393.
- A. Pohlkötter, U. Willer, C. Bauer, W. Schade, Resonant tuning fork detector for electromagnetic radiation, *Appl. Opt.* 48 (4) (2009) B119–B125.
- Y.F. Ma, Y. He, Y. Tong, X. Yu, F.K. Tittel, Quartz-tuning-fork enhanced photothermal spectroscopy for ultra-high sensitive trace gas detection, *Opt. Express* 26 (24) (2018) 32103–32110.
- X.N. Liu, Y.F. Ma, Sensitive carbon monoxide detection based on light-induced thermoelastic spectroscopy with a fiber-coupled multipass cell, *Chin. Opt. Lett.* 20 (3) (2022), 031201.
- L. Hu, C. Zheng, M. Zhang, K. Zheng, F.K. Tittel, Long-distance in-situ methane detection using near-infrared light-induced thermo-elastic spectroscopy, *Photoacoustics* 21 (2021), 100230.
- C.G. Lou, X.T. Li, H.J. Chen, X. Yang, Y. Zhang, J.Q. Yao, X.L. Liu, Polymer-coated quartz tuning fork for enhancing the sensitivity of laser-induced thermoelastic spectroscopy, *Opt. Express* 29 (8) (2021) 12195–12205.
- Y.Q. Hu, S.D. Qiao, Y. He, Z.T. Lang, Y.F. Ma, Quartz-enhanced photoacoustic-photothermal spectroscopy for trace gas sensing, *Opt. Express* 29 (4) (2021) 5121–5127.
- Y.F. Ma, Z.T. Lang, Y. He, S.D. Qiao, Y. Li, Ultra-highly sensitive hydrogen chloride detection based on quartz-enhanced photothermal spectroscopy, *Sensors* 21 (10) (2021) 3563.
- S.Z. Li, L. Dong, H.P. Wu, A. Sampaolo, P. Patimisco, V. Spagnolo, F.K. Tittel, Ppb-level quartz-enhanced photoacoustic detection of carbon monoxide exploiting a surface grooved tuning fork, *Anal. Chem.* 91 (9) (2019) 5834–5840.
- Y.F. Ma, Y. He, P. Patimisco, A. Sampaolo, S.D. Qiao, X. Yu, F.K. Tittel, V. Spagnolo, Ultra-high sensitive trace gas detection based on light-induced thermoelastic spectroscopy and a custom quartz tuning fork, *Appl. Phys. Lett.* 116 (1) (2020), 011103.
- S.D. Qiao, Y. He, Y.F. Ma, Trace gas sensing based on single-quartz-enhanced photoacoustic-photothermal dual spectroscopy, *Opt. Lett.* 46 (10) (2021) 2449–2452.
- H.P. Wu, A. Sampaolo, D. Lei, P. Patimisco, X.L. Liu, H.D. Zheng, X.K. Yin, W. G. Ma, L. Zhang, W.B. Yin, V. Spagnolo, S.T. Jia, F.K. Tittel, Quartz enhanced photoacoustic H<sub>2</sub>S gas sensor based on a fiber-amplifier source and a custom tuning fork with large prong spacing, *Appl. Phys. Lett.* 107 (11) (2015), 111104.
- I.E. Gordon, L.S. Rothman, C. Hill, R.V. Kochanov, Y. Tan, P.F. Bernath, M. Birk, V. Boudon, A. Campargue, K.V. Chance, B.J. Drouin, J.M. Flaud, R.R. Gamache, J. T. Hodges, D. Jacquemart, V.I. Perevalov, A. Perrin, K.P. Shine, M.A.H. Smith, J. Tennyson, G.C. Toon, H. Tran, V.G. Tyuterev, A. Barbe, A.G. Császár, V.M. Devi, T. Furtenbacher, J.J. Harrison, J.M. Hartmann, A. Jolly, T.J. Johnson, T. Karman, I. Kleiner, A.A. Kyuberis, J. Loos, O.M. Lyulin, S.T. Massie, S.N. Mikhailenko, N. Moazzen-Ahmadi, H.S.P. Müller, O.V. Naumenko, A.V. Nikitin, O.L. Polyansky, M. Rey, M. Rotger, S.W. Sharpe, K. Sung, E. Starikova, S.A. Tashkun, J. Vander-Auwera, G. Wagner, J. Wilzewski, P. Wcislo, S. Yu, E.J. Zak, The HITRAN 2016 molecular spectroscopic database, *J. Quant. Spectrosc. Radiat. Transf.* 203 (2017) 3–69.



**Shunda Qiao** received his B.S. degree in electronic science and technology from Yanshan university, China, in 2018. In 2020, he received his M.S. degree and began to pursue a Ph.D. degree of physical electronics from Harbin institute of technology. His research interests include photoacoustic spectroscopy and its applications.



**Angelo Sampaolo** obtained his Master degree in Physics in 2013 and the Ph.D. Degree in Physics in 2017 from University of Bari. He was a visiting researcher in the Laser Science Group at Rice University from 2014 to 2016. Since March 2021, he is assistant professor at the Polytechnic of Bari. His research activity has included the study of the thermal properties of heterostructured devices via Raman spectroscopy. Most recently, his research interest has focused on the development of innovative techniques in trace gas sensing, based on Quartz-Enhanced Photoacoustic Spectroscopy, Tunable Laser Diode Absorption Spectroscopy, Light-Induced Thermoelastic Spectroscopy and covering the full spectral range from near-IR to

THz. He is author of more than 100 Scopus publications and of more than 50 conference contributions. He is CEO and cofounder of PolySense Innovations.



**Pietro Patimisco** obtained the Master degree in Physics (cum laude) in 2009 and the Ph.D. Degree in Physics in 2013 from the University of Bari. Since 2018, he is Assistant professor at the Technical University of Bari. He was a visiting scientist in the Laser Science Group at Rice University in 2013 and 2014. Dr. Patimisco's scientific activity addressed both micro-probe optical characterization of semiconductor optoelectronic devices and optoacoustic gas sensors. Recently, his research activities included the study and applications of trace-gas sensors, such as quartz-enhanced photoacoustic spectroscopy and cavity enhanced absorption spectroscopy in the mid infrared and terahertz spectral region, leading to several publications, including a cover paper in *Applied Physics Letter* of the July 2013 issue.



**Vincenzo Spagnolo** received the Ph.D., both in physics, from University of Bari in 1994. He works as Full Professor of Applied Physics at the Technical University of Bari. In 2019, he became Vice-president of the Technical University of Bari, deputy to Technology Transfer. The main scientific activity of Vincenzo Spagnolo has been related the development of optoacoustic gas sensors based on quartz-enhanced photoacoustic spectroscopy. He has been visiting researcher at Rice University (Texas) in 2009 and 2010 and visiting professor in 2017. He is "hundred talents" visiting professor at Shanxi University in Taiyuan (China). Since 2017, he is the director of the joint-research lab PolySense, created by THORLABS GmbH and Technical University of Bari. His research activity is documented by more than 230 Scopus publications and three filed patents (more than 4500 citations, h-index 41). He has given more than 60 invited presentations at international conferences and workshops. Prof. Spagnolo is Fellow member of the SPIE and senior member of the Optica.



**Yufei Ma** received his Ph.D. degree in physical electronics from Harbin Institute of Technology, China, in 2013. From September 2010 to September 2011, he spent as a visiting scholar at Rice University, USA. Currently, he is a professor at Harbin Institute of Technology, China. He is the winner of National Outstanding Youth Science Fund. His research interests include optical sensors, trace gas detection, laser spectroscopy, solid-state laser and optoelectronics. He has published more than 100 publications and given more than 20 invited presentations at international conferences. He serves as associate editor for *Optica*, *Optics Express*, *SPIE Optical Engineering*, *Wiley Microwave and Optical Technology Letters* and *Frontiers in Physics*. He also serves as topical editor for *CLP Chinese Optics Letters* and editorial board member for *MDPI Sensors*, *Applied Sciences* and Elsevier *Photoacoustics*.